SCALE EFFECTS IN MEDIA WITH PERIODIC AND NEARLY PERIODIC MICROSTRUCTURES — I. MACROSCOPIC PROPERTIES

by:

M. SCHRAAD and N. TRIANTAFYLLIDIS

Published in the: Journal of Applied Mechanics, 1997, Volume 64, pp.751-762

SCALE EFFECTS IN MEDIA WITH PERIODIC AND NEARLY PERIODIC MICROSTRUCTURES — I. MACROSCOPIC PROPERTIES

by:

M. SCHRAAD and N. TRIANTAFYLLIDIS

Department of Aerospace Engineering

The University of Michigan

Ann Arbor, Michigan 48109-2118

Abstract

Traditional averaging and homogenization techniques, developed to predict the macroscopic properties of heterogeneous media, typically ignore microstructure related scale effects — that is, the influence of the size of the representative volume, relative to the size of the unit cell. This issue is presently investigated by exploring the behavior of a nonlinearly elastic, planar, lattice model, which is subjected to general macroscopic deformations. For these materials, scale effects may be due to nonuniformities in the macroscopic strain field throughout the specimen, or alternatively, to the presence of microstructural imperfections that may be either geometric or constitutive in nature. For the case of macroscopic strain nonuniformities, it is shown that the microstructure related scale effects can be accounted for by the presence of higher order gradient terms in the macroscopic strain energy density of the model. For the case of microstructural imperfections, the difference between the respective macroscopic properties of the perfect and imperfect models are shown to depend on the relative size of the specimen, and on the imperfection amplitude and wavelength, while being nearly insensitive to the imposed macroscopic strain. For all of the cases considered, several analytical approximations are proposed to predict the influence of scale on the macroscopic properties, and the accuracy of each method is examined.

1 INTRODUCTION

The standard approach to the design of any structure, requires a continuum description of the engineering material that will be used for its fabrication. Modern material science can tailor, to an unprecedented degree, the microstructure of engineering materials to give them the desired macroscopic properties. In response to these technological advances, there has been a renewed and strong interest in solid mechanics for predicting the macroscopic (continuum) properties of engineering materials based on their microstructure. The corresponding methodologies are frequently termed "*averaging*" or "*homogenization*" techniques.

There is voluminous literature in engineering and applied physics, spanning well over a hundred years of research, which is devoted primarily to the averaging or homogenization problem involved in predicting the macroscopic properties of linearly elastic materials under small strains. For these problems, the microgeometries considered are general, and countless averaging techniques, both deterministic and statistical, have been developed to date. In addition, beginning with the work of Voigt (1889), various bounding techniques have also been developed to give accurate estimates of the overall properties of elastic composites. All of these methods have subsequently been extended to include more general constitutive laws, ranging from small strain elasto-plasticity (see Hill, 1965), to finite strain elasticity (see Talbot and Willis, 1985). All of these classical averaging techniques ignore the "*scale effect*" (i.e., the influence of the size of the representative volume, relative to the characteristic length of the underlying microstructure). The quantification of this scale effect, however, is important to a variety of technological applications, including dispersion in wave propagation problems, current problems involving nanoscale sized structures, and the prediction of localized failure mechanisms in composites, to state only a few.

To correct this deficiency, a number of phenomenological remedies have been proposed, which involve the relaxation of the "*local action*" hypothesis of classical continuum mechanics. This hypothesis dictates that only the first gradient of the deformation enters the constitutive law. Continuum models that violate the local action hypothesis are termed "*non-local*", and can be classified into several different categories: micropolar or "*Cosserat*" type models, integral type models, and higher order gradient type models. Although the majority of the previously mentioned averaging techniques are phenomenological, some effort has recently been dedicated to deriving macroscopic higher order gradient theories based on micromechanical models. For the case of linear elasticity, the microgeometries considered in these derivations are general (see Drugan and Willis, 1996). In addition, for the case of nonlinear materials under finite deformations, analogous non-local models have recently been derived for periodic media (see Bardenhagen and Triantafyllidis, 1994, for materials with discrete microstructures, and Triantafyllidis

and Bardenhagen, 1997, for microstructured continua).

The present work is motivated by engineering applications involving periodic, and nearly periodic, ductile composites, under finite macroscopic strains. Of interest here is the quantification of the scale effect on the macroscopic properties and the failure mechanisms of these materials. For this class of applications one can unambiguously identify a scale parameter, which characterizes the size of the specimen, relative to the characteristic microstructural length. To quantify the above mentioned scale effects under general finite macroscopic strains, a simple model is proposed, for which the microstructure is idealized as a nonlinear, planar, lattice model, with a square, six-element unit cell. The first part of this work explores the influence of scale on the overall properties of the lattice models. The second part investigates the microstructure related scale effects on the onset of failure in these materials.

More specifically, in the first part of this work, the influence of scale on the macroscopic properties of the material are investigated at finite levels of strain. For the perfectly periodic model, there is only one relevant scale, characterized by the "*geometric*" scale parameter ϵ, which is defined to be the ratio of the size of the unit cell h, to the size of the representative volume H on which the macroscopic properties are defined. The macroscopic energy density W, for models with perfectly periodic microstructure, depends solely on the imposed macroscopic deformation gradient $\mathbf{F}$, and is independent of the geometric scale parameter ϵ. In engineering applications there are two different sources for the scale dependence of the macroscopic properties: the nonuniformity of the imposed macroscopic strain, and the imperfections which are inevitably present in any nearly periodic composite, due to inaccuracies in the manufacturing process. The scale parameters, resulting from the strain gradient and microstructural imperfections, are related to the geometric scale parameter ϵ. Consequently, a strain gradient parameter κ, and an imperfection amplitude parameter δ are defined, where κH and $\delta\epsilon$ are the dimensionless "*deformation*" and "*imperfection*" scale parameters, respectively. The scale dependence of the macroscopic quantities (i.e., the strain energy density, the stresses, and the incremental moduli) is made explicit through their dependence on the parameters ϵ, κ, and δ.

Detailed numerical investigations are conducted to determine the influence of both the deformation and imperfection scale parameters on the macroscopic properties of the lattice models. To study the effects of nonuniform strains, bending deformations, which are superimposed onto the uniform uniaxial strains, are considered. Here, the influence of scale is explored by examining the strain energy density of the material. To study the effects of microstructural imperfections, two different types are considered: geometric and constitutive. In addition, for each type of imperfection, the amplitude is held constant, and the effects of various regular, as well as random imperfection shapes are examined. In this case, the scale effects are quantified through a scalar parameter which measures the stress deviation of the

imperfect model from its perfectly periodic counterpart.

Moreover, in the interest of gaining additional insight into how the macroscopic properties are influenced by the strain gradient and imperfection amplitude parameters, analytical approximations are proposed for small values of κ and δ. For each case investigated, the analytical results of the proposed approximations are compared with the results of numerical calculations involving the exact equilibrium equations of the entire micromechanical model. The proposed analytical approximations are accurate for adequately large values of κ and δ, and for finite macroscopic strains. As expected, these approximations break down once an instability strain is approached (for details, see Part II of this work).

The presentation is concluded with a detailed discussion of the results pertaining to scale effects on the macroscopic properties. Issues concerning the onset of failure for the lattice models, and the corresponding microstructure related scale effects, are the subject of the investigation in Part II.

2 MODEL DESCRIPTION

Consider the discrete, planar, lattice model, shown in Figure 1a. This model, which is a representative volume of a larger microstructured medium, is a perfectly periodic assembly of unit cells. In the reference (undeformed) configuration these unit cells are squares, each cell having common dimensions $h \times h$, where h is the characteristic microstructural length of the material. The geometric scale parameter ϵ is defined as the ratio of this characteristic microstructural length h, to the length H that defines the size of the representative volume ($V = H \times H$). For convenience, the representative volume dimension H is set equal to unity for all models. Therefore, $\epsilon = h/H = 1/N$, where N is the number of unit cells in each row or column of the representative volume. If the cross-sectional areas of the model elements are scaled appropriately, this is equivalent to fixing the unit cell dimensions, and varying the size of the representative volume.

Each of the unit cells consists of four nodes (one at each vertex) connected by six one-dimensional, nonlinearly elastic elements. Each node possesses two translational degrees of freedom and is capable of transmitting forces, but cannot transmit moments. As a result, the elements are stressed axially, but do not support shear forces or bending moments.

The reference position vector (in the undeformed configuration) for each node is denoted by $\mathbf{X}$ and the current position vector (in the deformed configuration) is denoted by $\mathbf{x}$. The relative position vector of the nodes for each element is defined by $\Delta\mathbf{X} = \epsilon\boldsymbol{\Delta}$ in the reference configuration and by $\Delta\mathbf{x} = \epsilon\boldsymbol{\Delta} + \Delta\mathbf{u}$ in the current configuration. Here, $\boldsymbol{\Delta}$ is the dimensionless relative position vector of the element nodes in the reference configuration, and $\Delta\mathbf{u}$ is the relative displacement vector of the element nodes in the current configuration. Therefore, the element length in the reference configuration L is given by

$$L = (\Delta\mathbf{X}\cdot\Delta\mathbf{X})^{\frac{1}{2}} = \epsilon\,(\boldsymbol{\Delta}\cdot\boldsymbol{\Delta})^{\frac{1}{2}}\,, \tag{1}$$

and the element length in the current configuration l is given by

$$l = (\Delta\mathbf{x}\cdot\Delta\mathbf{x})^{\frac{1}{2}}\,. \tag{2}$$

Due to the finite deformations of the lattice models, nonlinear kinematic relations are required. In one dimension, all nonlinear strain measures are equivalent. Here, for convenience, the Lagrangian strain e is adopted:

$$e = \frac{1}{2}\left[\left(\frac{l}{L}\right)^2 - 1\right]. \tag{3}$$

The element strain energy $\mathcal{E}$ is taken to be

$$\mathcal{E} = AEL\left[\frac{1}{2}e^2 + (\text{sgn } e)\,\frac{1}{3}ae^3 + \frac{1}{4}be^4\right], \tag{4}$$

where $A = \mathcal{A}\epsilon$ is the cross-sectional area of the element, E is the initial tangent modulus of the material, and the quantities a and b are material constants. The cross-sectional areas of the elements scale with the size of the unit cell to provide a stress-strain response which is independent of the geometric scale parameter ϵ, for all perfectly periodic models. The nondimensional force (f/EA) versus elongation $((l-L)/L)$ response (where $f = d\mathcal{E}/dl$) for the base element of the unit cell with $\mathcal{A} = 1$, $E = 1$, $a = -7/2$ and $b = 7/2$, is shown in Figure 1b. These constants are adopted here, and for all subsequent applications, because they give rise to a macroscopic stress-strain response with a broad nonlinear range, and a maximum load at a finite level of strain for all the load paths considered.

The lattice models are subjected to general in-plane deformations, where the displacement vector $\mathbf{u}$ of each constrained node corresponds to a linearly varying, continuous, macroscopic deformation gradient $\mathbf{F}(\mathbf{X})$:

$$\mathbf{u} = (\mathbf{F}_0 - \mathbf{I})\cdot\mathbf{X} + \frac{1}{2}\mathbf{X}\cdot\mathbf{F}_1\cdot\mathbf{X}, \qquad \text{where} \qquad \mathbf{I} + \mathbf{u}\otimes\nabla = \mathbf{F}(\mathbf{X}) = \mathbf{F}_0 + \mathbf{F}_1\cdot\mathbf{X}. \tag{5}$$

Here, $\mathbf{F}_0 = (1/V)\int_V \mathbf{F}(\mathbf{X})\,dV$ is the average macroscopic deformation gradient tensor, and $\mathbf{F}_1 = \mathbf{F}\otimes\nabla$ is the (constant) second order deformation gradient tensor which characterizes the nonuniformity of the macroscopic strain in the representative volume of the material. In addition to the geometric scale parameter ϵ, which characterizes the relative size of the specimen under investigation, a deformation scale parameter, which characterizes the spatial variations in the imposed strain field, can be defined by the dimensionless parameter κH. Here, κ is the strain gradient parameter defined to be the norm of the second order deformation gradient tensor (i.e., $\kappa \equiv \|\mathbf{F}\otimes\nabla\| = [(\mathbf{F}\otimes\nabla)_{ijk}(\mathbf{F}\otimes\nabla)_{ijk}]^{1/2}$).

The average deformation gradient tensor $\mathbf{F}_0$ can be decomposed into the product of the tensor of principal stretch ratios $\mathbf{U}$, and an orientation tensor $\mathbf{R}$, such that

$$\mathbf{F}_0 = \mathbf{R}^T\cdot\mathbf{U}\cdot\mathbf{R}, \tag{6}$$

where

$$\mathbf{U} = \begin{bmatrix} \lambda_1 & 0 \\ 0 & \lambda_2 \end{bmatrix} \qquad \text{and} \qquad \mathbf{R} = \begin{bmatrix} \cos\theta & \sin\theta \\ -\sin\theta & \cos\theta \end{bmatrix}, \tag{7}$$

and where θ indicates the orientation of the principal strains with respect to the initial axes of material orthotropy. The principal stretch ratios λ_1 and λ_2 are parameterized in terms of a single load parameter λ and a load path angle ϕ:

$$\lambda_1 = 1 + \lambda\cos\phi \qquad \text{and} \qquad \lambda_2 = 1 + \lambda\sin\phi. \tag{8}$$

Thus, setting $\theta = 0$, and letting ϕ range from 0 to 2π, all possible orthotropic deformations, which involve all combinations of biaxial tension and compression, are produced. Various amounts of shear are superimposed by letting θ vary between 0 and $\pi/2$, thereby encompassing all possible macroscopic deformations.

To investigate the influence of microstructural imperfections on the macroscopic properties of the model, the initially periodic microstructural geometry and the initially uniform element material properties of the lattice are perturbed. For each type of imperfection, both regular and random shapes are considered. An imperfection scale parameter, which characterizes the relative size of the imperfection in the material microstructure, can be defined by the dimensionless parameter $\delta\epsilon$, where δ is the corresponding imperfection amplitude parameter.

For example, "*geometric*" imperfections are produced by perturbing the initially periodic internal nodal position vectors. A regular imperfection in the reference position vector $\mathbf{X} = (X_1, X_2)$ of an interior node is given by the new perturbed reference position vector $\overline{\mathbf{X}}$, defined by

$$\overline{\mathbf{X}} = \mathbf{X} + \delta\epsilon H \sin\left[\frac{m_1\pi}{H}\left(X_1 + \frac{H}{2}\right)\right] \sin\left[\frac{m_2\pi}{H}\left(X_2 + \frac{H}{2}\right)\right](\mathbf{e}_1 + \mathbf{e}_2)\,, \tag{9}$$

while a random imperfection is produced by

$$\overline{\mathbf{X}} = \mathbf{X} + \delta\epsilon H\,(r_1\mathbf{e}_1 + r_2\mathbf{e}_2)\,. \tag{10}$$

Here, m_1 and m_2 are the wave numbers of the regular imperfection shape, and r_1 and r_2 are random numbers between -1 and 1.

"*Constitutive*" imperfections are produced by perturbing the initially uniform internal element cross-sectional areas. A regular imperfection in the cross-sectional area $A = \mathcal{A}\epsilon$ of an interior element centered at (X_1, X_2) is given by the new perturbed cross-sectional area $\overline{A}$, defined by

$$\overline{A} = \mathcal{A}\epsilon\left\{1 + \delta\sin\left[\frac{m_1\pi}{H}\left(X_1 + \frac{H}{2}\right)\right]\sin\left[\frac{m_2\pi}{H}\left(X_2 + \frac{H}{2}\right)\right]\right\}, \tag{11}$$

while a random imperfection is produced by

$$\overline{A} = \mathcal{A}\epsilon\left(1 + \delta r\right), \tag{12}$$

where r is, again, a random number between -1 and 1. These imperfections affect the constitutive law of each element, and are equivalent to similar imperfections involving the initial tangent modulus of the material E, or the material constants a and b.

Notice that for both types of imperfection, the boundary nodes are kept in their initially perfect positions, and the elements which lie on the model boundaries maintain their originally uniform cross-sectional areas. As an example, the reference configurations for planar lattice models with $\epsilon = 0.1$ and regular ($m_1 = m_2 = 2$) and random geometric imperfections are shown in Figure 2a and Figure 2b, respectively. Here, the imperfection amplitude parameter for both imperfection shapes is $\delta = 0.25$.

3 MACROSCOPIC PROPERTIES

The macroscopic properties of the planar lattice are defined on the representative volume of the model. For problems involving nonuniform deformations, linearly varying strain fields are imposed by prescribing displacements at every node in the lattice model. The resulting strain energy density is found in terms of the average and second order deformation gradient tensors $\mathbf{F}_0$ and $\mathbf{F}_1$, respectively. For problems involving microstructural imperfections, displacements corresponding to uniform deformations are prescribed on the boundaries of the representative volume, and the equilibrium strain energy density is determined in terms of the average deformation gradient tensor $\mathbf{F}_0$, and the imperfection amplitude parameter δ.

The exact strain energy density W is defined to be the representative volume average of the total strain energy $\mathcal{E}$, which is the sum of the element strain energies $\mathcal{E}^{el}$:

$$W = \frac{1}{V}\mathcal{E} = \frac{1}{V}\sum_{cell=1}^{N^2}\left[\sum_{el=1}^{6}\mathcal{E}^{el}\left(e^{el}\right)\right]_{cell}. \tag{13}$$

This exact strain energy density is used to determine the exact macroscopic first Piola-Kirchhoff stress tensor $\mathbf{\Pi}$, which is defined by

$$\mathbf{\Pi}^T = \frac{\partial W}{\partial \mathbf{F}_0} = \frac{1}{V}\sum_{cell=1}^{N^2}\left[\sum_{el=1}^{6}\frac{\partial \mathcal{E}^{el}}{\partial \mathbf{u}}\cdot\frac{\partial \mathbf{u}}{\partial \mathbf{F}_0}\right]_{cell}, \tag{14}$$

and the exact macroscopic incremental moduli tensor $\mathbf{L}$, which is given by

$$\mathbf{L} = \frac{\partial^2 W}{\partial \mathbf{F}_0 \partial \mathbf{F}_0} = \frac{1}{V}\sum_{cell=1}^{N^2}\left[\sum_{el=1}^{6}\frac{\partial \mathbf{u}}{\partial \mathbf{F}_0}\cdot\frac{\partial^2 \mathcal{E}^{el}}{\partial \mathbf{u}\partial \mathbf{u}}\cdot\frac{\partial \mathbf{u}}{\partial \mathbf{F}_0}\right]_{cell}. \tag{15}$$

The simplification of the second derivative of the total strain energy with respect to the average deformation gradient tensor $\partial^2\mathcal{E}/\partial\mathbf{F}_0\partial\mathbf{F}_0$ in equation (15) is made as follows. Consider the equilibrium equations,

$$\delta\mathbf{u}\cdot\frac{\partial \mathcal{E}}{\partial \mathbf{u}} = 0 \qquad \text{in} \qquad V \qquad \text{and} \qquad \delta\mathbf{u} = \mathbf{0} \qquad \text{on} \qquad \partial V, \tag{16}$$

where ∂V denotes the boundary of the representative volume. Since the second derivative of the displacement vector with respect to the average deformation gradient tensor $\partial^2\mathbf{u}/\partial\mathbf{F}_0\partial\mathbf{F}_0$ is a kinematically admissible field (i.e., $\mathbf{u} = (\mathbf{F}_0 - \mathbf{I})\cdot\mathbf{X}$ on $\partial V \Rightarrow \partial^2\mathbf{u}/\partial\mathbf{F}_0\partial\mathbf{F}_0 = \mathbf{0}$ on ∂V), it follows from equation (16) that

$$\frac{\partial^2 \mathcal{E}}{\partial \mathbf{F}_0 \partial \mathbf{F}_0} = \frac{\partial \mathbf{u}}{\partial \mathbf{F}_0} \cdot \frac{\partial^2 \mathcal{E}}{\partial \mathbf{u} \partial \mathbf{u}} \cdot \frac{\partial \mathbf{u}}{\partial \mathbf{F}_0}. \tag{17}$$

The derivative of the displacement vector with respect to the average deformation gradient tensor $\partial \mathbf{u}/\partial \mathbf{F}_0$ in equations (14) and (15) is found by taking the derivative of the equilibrium equations with respect to the average deformation gradient tensor,

$$\delta \mathbf{u} \cdot \frac{\partial^2 \mathcal{E}}{\partial \mathbf{u} \partial \mathbf{u}} \cdot \frac{\partial \mathbf{u}}{\partial \mathbf{F}_0} = \mathbf{0} \qquad \text{in} \qquad V \qquad \text{and} \qquad \frac{\partial \mathbf{u}}{\partial \mathbf{F}_0} = \mathbf{X} \qquad \text{on} \qquad \partial V, \tag{18}$$

and solving the resulting equations for $\partial \mathbf{u}/\partial \mathbf{F}_0$.

For the case of a lattice model with perfectly periodic microstructure ($\delta = 0$), subjected to uniform deformations ($\mathbf{F} \otimes \nabla = \mathbf{0}$), the macroscopic properties W, $\mathbf{\Pi}$, and $\mathbf{L}$ do not depend on ϵ, that is, on the relative size of the representative volume. However, when spatial variations in the strain field are imposed or microstructural imperfections are present, the macroscopic properties depend on the geometric scale parameter ϵ, the strain gradient parameter κ, and the imperfection amplitude parameter δ.

The goals of the present work are threefold. First, to study the influence of scale, due to nonuniform deformations, on the exact strain energy density of the perfectly periodic lattice models. Second, to investigate the influence of scale, due to microstructural imperfections, on the macroscopic stress-strain response of the nearly periodic lattice models. And third, to derive analytical approximations for the macroscopic properties of lattice models which are subjected to nonuniform deformations or possess geometric and constitutive microstructural imperfections, and to compare these approximations with their exact counterparts.

3.1 APPROXIMATION FOR NONUNIFORM DEFORMATIONS

Consider a planar lattice model with perfectly periodic microstructure ($\delta = 0$), subjected to overall, nonuniform deformations ($\mathbf{F} \otimes \nabla \neq \mathbf{0}$). The scale effects, which are due to the spatial variations in the strain field within the representative volume, are approximated by considering the asymptotic expansion of the exact strain energy density. The expansion used here is based on an extension of the continuum calculations of Born and Huang (1954) for the elastic properties of perfect crystals. These continuum calculations, involving only first order gradient terms, result in an expression for the strain energy density which neglects the characteristic microstructural length, and its role in determining the overall behavior of the material. Bardenhagen and Triantafyllidis (1994) have extended this formulation to include higher order gradient terms, which result in an energy density that depends on the geometric scale parameter ϵ.

Following this higher order gradient method, the current relative position vector of the element nodes can be expanded, using the Taylor series, as

$$\Delta\mathbf{x} = \epsilon\mathbf{F}\cdot\boldsymbol{\Delta} + \frac{\epsilon^2}{2}\left(\mathbf{F}\otimes\nabla\right) : \left(\boldsymbol{\Delta}\otimes\boldsymbol{\Delta}\right) + O\left(\epsilon^3\right). \tag{19}$$

Substitution of the expansion (19) and the kinematic relations (1) – (3) into the definition of the strain energy density (13), and subsequent expansion of the result in terms of ascending powers of the geometric scale parameter ϵ, yields

$$W = \frac{1}{V}\int_V \left[\overline{W} + \frac{\epsilon^2}{2}\left(\mathbf{F}\otimes\nabla\right) \vdots\mathbf{B}\vdots \left(\mathbf{F}\otimes\nabla\right) + O\left(\epsilon^4\right)\right] dV, \tag{20}$$

where $\overline{W}$ is defined by

$$\overline{W}\left(\mathbf{F}\right) = \frac{1}{V}\sum_{el=1}^{6} \mathcal{E}^{el}\left(\overline{e}^{el}\left(\mathbf{F}\right)\right), \tag{21}$$

and the average element strain $\overline{e}^{el}$ is given by

$$\overline{e}^{el}\left(\mathbf{F}\right) = \frac{1}{2}\left[\frac{\left(\mathbf{F}\cdot\boldsymbol{\Delta}^{el}\right)\cdot\left(\mathbf{F}\cdot\boldsymbol{\Delta}^{el}\right)}{\boldsymbol{\Delta}^{el}\cdot\boldsymbol{\Delta}^{el}} - 1\right]. \tag{22}$$

In addition, the components of the tensor $\mathbf{B}$ are found, from the same expansion, to be

$$B_{ijklmn} = -\frac{1}{12}\frac{1}{V}\sum_{el=1}^{6}\left\{\frac{\partial^2\mathcal{E}^{el}\left(\overline{e}^{el}\left(\mathbf{F}\right)\right)}{\partial\overline{e}^{el\,2}}\frac{F_{ip}\Delta_p^{el}F_{lq}\Delta_q^{el}}{\left(\boldsymbol{\Delta}^{el}\cdot\boldsymbol{\Delta}^{el}\right)^2} + \frac{\partial\mathcal{E}^{el}\left(\overline{e}^{el}\left(\mathbf{F}\right)\right)}{\partial\overline{e}^{el}}\frac{\delta_{il}}{\boldsymbol{\Delta}^{el}\cdot\boldsymbol{\Delta}^{el}}\right\}\Delta_j^{el}\Delta_k^{el}\Delta_m^{el}\Delta_n^{el}. \tag{23}$$

The second order ($O(\epsilon^2)$) and higher order terms in the continuum expression for the macroscopic strain energy density depend on the relative size of the representative volume. The fact that more than one continuum strain energy density can be found for the same discrete model is a known phenomenon in mathematical physics (see, for example, the discussion in Kunin, 1982). The various continuum strain energy densities, which differ by a null Lagrangian, produce identical Euler-Lagrange (equilibrium) equations as discussed in Triantafyllidis and Bardenhagen (1993) for one-dimensional; and Bardenhagen and Triantafyllidis (1994) for two- and three-dimensional, nonlinearly elastic lattice networks. It will be shown that the exact strain energy density of the representative volume converges, within an accuracy of $O(\epsilon^4)$, to the continuum approximation given in equation (20), thus justifying the particular choice for the $O(\epsilon^2)$ term used in that expression. The proof of the corresponding convergence result for the simpler, one-dimensional lattice model is given in Appendix A.

3.2 APPROXIMATIONS FOR MICROSTRUCTURAL IMPERFECTIONS

Next, consider a planar lattice model, with either geometric or constitutive microstructural imperfections ($\delta \neq 0$), subjected to boundary displacements which correspond to uniform macroscopic deformations ($\mathbf{F} \otimes \nabla = \mathbf{0}$). These microstructural imperfections cause spatial variations in the strain field which affect the macroscopic properties of the material. Three different approximations, which estimate the effects of these imperfections on the macroscopic properties, will be considered, and the macroscopic stress-strain response predicted by these approximations will be compared to the exact solution.

The first approximation, is the standard "*Voigt*" approximation (see Voigt, 1889), which uses the average deformation gradient tensor $\mathbf{F}_0$ in place of the actual macroscopic deformation gradient tensor $\mathbf{F}(\mathbf{X})$ in the definition (13) for the strain energy density. Therefore, the approximate strain energy density becomes

$$\overline{W}_V = W(\delta, \mathbf{F}_0), \tag{24}$$

and the approximate macroscopic stress and incremental moduli tensors are defined in the same manner that was given in equations (14) and (15), respectively, where the use of the average macroscopic deformation gradient tensor in place of the actual deformation gradient tensor is retained.

The second approximation is a standard linearization approximation, according to which the macroscopic properties are expanded about the perfect solution. Terms higher than first order in the imperfection amplitude parameter δ are neglected, resulting in approximate macroscopic properties that are linear in the imperfection amplitude parameter. For the strain energy density, this approximation gives

$$\overline{W}_L = W_0 + \delta W_1; \qquad W_0 = W|_{\delta=0} \qquad \text{and} \qquad W_1 = \left.\frac{dW}{d\delta}\right|_{\delta=0}, \tag{25}$$

where W_0 is the strain energy density of the perfectly periodic model. Similarly, the macroscopic stress tensor of the imperfect model, as derived by the linearization approximation, is given by

$$\overline{\mathbf{\Pi}}_L = \mathbf{\Pi}_0 + \delta \mathbf{\Pi}_1; \qquad \mathbf{\Pi}_0^T = \frac{1}{V}\left(\frac{\partial \mathcal{E}}{\partial \mathbf{u}} \cdot \frac{\partial \mathbf{u}}{\partial \mathbf{F}_0}\right)\bigg|_{\delta=0} \qquad \text{and} \qquad \mathbf{\Pi}_1^T = \frac{1}{V}\left(\frac{\partial^2 \mathcal{E}}{\partial \mathbf{u} \partial \delta} \cdot \frac{\partial \mathbf{u}}{\partial \mathbf{F}_0}\right)\bigg|_{\delta=0}, \tag{26}$$

where $\mathbf{\Pi}_0$ is the macroscopic stress tensor of the perfectly periodic model. In addition, similar expressions can be found for the approximate macroscopic incremental moduli tensor.

The third, and last approximation considered, is an improvement of the previously mentioned standard linearization approximation, and is termed the displacement linearization approximation. According to

this approximation, only the displacement field is expanded about the perfect solution, and terms higher than first order in the imperfection amplitude parameter δ are neglected, resulting in an approximate displacement field that is linear in the imperfection amplitude parameter. For the strain energy density, this approximation gives

$$\overline{W}_{DL} = W\left(\delta, \mathbf{u}_L\left(\delta\right)\right). \tag{27}$$

Here, the displacement field is approximated as

$$\mathbf{u}_L\left(\delta\right) = \mathbf{u}_0 + \delta\mathbf{u}_1; \qquad \mathbf{u}_0 = \mathbf{u}|_{\delta=0} \qquad \text{and} \qquad \mathbf{u}_1 = \left.\frac{d\mathbf{u}}{d\delta}\right|_{\delta=0}, \tag{28}$$

where $\mathbf{u}_0$ is the uniform displacement field of the perfectly periodic model. Again, the macroscopic stress and incremental moduli tensors are defined in the same manner that was given in equations (14) and (15), respectively, where the use of the linearized displacement field in place of the exact displacement field is retained.

It should be mentioned, once again, at this point, that certain simplifications must be made to obtain equation (26). Equilibrium is, again, considered and arguments similar to those presented in equations (16) – (18) are used to make these simplifications.

Two interesting and general results are obtained by considering the asymptotic expansion of the macroscopic properties. For models with arbitrary geometric imperfections, the first order terms in the expansions of the macroscopic properties are identically zero for all deformations satisfying the prescribed displacement boundary conditions (see Appendix B). Since the first order terms are zero (i.e., the effects of geometric imperfections are second order in the imperfection amplitude parameter δ), the linearization approximation gives the macroscopic properties of the perfectly periodic model as an approximation for the macroscopic properties of the imperfect model.

Furthermore, for models with either geometric or constitutive microstructural imperfections, the respective macroscopic properties of the lattice models, as predicted by the Voigt and the linearization approximations, differ only by terms that are second order in the imperfection amplitude parameter δ (see Appendix C). Therefore, the standard linearization approximation does not provide any additional information beyond that which is already known from the solution for the perfectly periodic model, or can be obtained, to the first order, from the Voigt approximation.

4 RESULTS

Analyses have been performed for lattice models with various geometric scale parameters and microstructural imperfections, subjected to different uniform and nonuniform deformations. Results are presented which illustrate the more typical microstructure related scale effects on the macroscopic properties of the planar lattice models. The material parameters used for the base element of the perfect unit cell in these analyses were given in Section 2 (see also Figure 1b).

Scale effects, which are due to nonuniform deformations, are studied first by examining the influence of linearly varying strain fields (i.e., strain fields with constant second order deformation gradient tensor $\mathbf{F}_1$), on the exact strain energy density of perfectly periodic lattice models with geometric scale parameters ranging from $\epsilon = 1.00$ to $\epsilon = 0.04$ ($N = 1$ to $N = 25$). The exact strain energy density is also compared to the approximate strain energy density, derived in Section 3.1. Next, scale effects, which are due to microstructural imperfections, are explored by studying the differences in the exact macroscopic stress-strain response of models with perfectly periodic microstructures and their counterparts with geometrically irregular and constitutively nonuniform microstructures. For models with imperfect microstructures, the macroscopic properties depend on the geometric scale parameter ϵ, the imperfection amplitude parameter δ, the imperfection shape (defined by the wave numbers m_1 and m_2 for regular imperfections), and the imposed macroscopic deformation (defined by the principal stretch ratios λ_1 and λ_2, and the orientation angle θ). Studies concerning the influence of each one of these parameters on the macroscopic stress-strain response of the imperfect lattice models are presented.

Lastly, the predictions for the macroscopic stress-strain response of models with imperfect microstructures, obtained using the Voigt and the displacement linearization approximations, are investigated and compared to the exact solutions. It should also be mentioned here that all the convergence statements made below, refer to apparent convergence based upon the relevant numerical results.

4.1 SCALE EFFECTS DUE TO NONUNIFORM DEFORMATIONS

To investigate the scale effects on the macroscopic properties of the representative volume, which result from imposing spatially varying strain fields, the exact strain energy density W is determined for a perfectly periodic model subjected to various macroscopically nonuniform deformations. The exact strain energy density is then compared to its approximate continuum counterpart obtained from the expansion given in equation (20). Of interest here, is the convergence of the exact strain energy density to its continuum average as the geometric scale parameter ϵ approaches zero.

To measure the accuracy of the first correction due to the imposed strain gradient, that is, the accuracy

of the $O(\epsilon^2)$ term in equation (20), a function $f(\epsilon)$ is defined as

$$f(\epsilon) = \frac{W - (1/V)\int_V \overline{W} dV}{(\epsilon^2/2)(\mathbf{F}\otimes\nabla)\vdots(1/V)\int_V \mathbf{B} dV \vdots (\mathbf{F}\otimes\nabla)}. \tag{29}$$

According to equation (20), the numerator in equation (29) is $O(\epsilon^2)$, and since the exact strain energy density converges to its continuum average as the relative size of the representative volume increases, the function $f(\epsilon)$ should converge to one as the geometric scale parameter ϵ approaches zero (recall the discussion in Section 3.1 regarding the correct $O(\epsilon^2)$ term, and the derivation in Appendix A of this term for a one-dimensional model).

Several different values for the average and second order deformation gradient tensors $\mathbf{F}_0$ and $\mathbf{F}_1$ have been considered. Some typical results are depicted in Figure 3 and correspond to the macroscopic deformation defined by

$$\mathbf{F}_0 = \begin{bmatrix} 1.05 & 0 \\ 0 & 1 \end{bmatrix}, \qquad (\mathbf{F}\otimes\nabla)_{122} = \kappa \qquad \text{and all other} \qquad (\mathbf{F}\otimes\nabla)_{ijk} = 0, \tag{30}$$

where the macroscopic strain gradient parameter is defined as the norm of the second order deformation gradient tensor $\kappa \equiv \|\mathbf{F}\otimes\nabla\|$. The second order deformation gradient considered in equation (30) adds bending to the uniform uniaxial strain defined by $\mathbf{F}_0$, as shown by the deformed configuration in the inset of Figure 3a for $\kappa H = 2.5$ (a relatively high value of the deformation scale parameter used to show the effects of $\mathbf{F}\otimes\nabla$). Figure 3a shows the scale effects associated with the resulting nonuniform deformation on the exact strain energy density of a perfectly periodic lattice model, and Figure 3b shows the corresponding convergence of the function $f(\epsilon)$ for values of the dimensionless deformation scale parameter ranging from $\kappa H = 0.025$ (solid line) to $\kappa H = 0.100$ (dotted line).

As expected, the results show that as the geometric scale parameter approaches zero, the exact strain energy density of the lattice model converges to its continuum average, and therefore, the function $f(\epsilon)$ converges to one. Notice that the convergence of the strain energy density is quite rapid, and that the accuracy of the second order term in the continuum expansion of the strain energy density at predicting the difference between the exact value and its continuum average improves as the relative size of the representative volume increases.

4.2 SCALE EFFECTS DUE TO MICROSTRUCTURAL IMPERFECTIONS

To investigate the scale effects on the macroscopic properties of the lattice, which are associated with the presence of imperfections in the microstructure, the exact macroscopic stress-strain response of a

model with perfectly periodic microstructure is compared to the exact response of models with geometric and constitutive microstructural imperfections. For example, Figure 4 shows the effects of a regular ($m_1 = m_2 = 1$) and a random constitutive imperfection (dashed and dotted lines, respectively) of twenty-five percent amplitude ($\delta = -0.25$) on the macroscopic stress-strain response of an initially periodic lattice model with $\epsilon = 0.04$ (solid line), subjected to uniaxial extension with no lateral contraction ($\phi = \theta = 0$ in equations (7) and (8)). For models with microstructural imperfections, the range of deformation is limited by the onset of failure, which is defined as the first maximum load encountered along the principal equilibrium path. An investigation of the influence of scale on the onset of failure for this model is presented in Part II of this work.

For lattice models with microstructural imperfections, the macroscopic properties depend on the geometric scale parameter ϵ, as well as on the imperfection amplitude parameter δ, the imperfection shape, and the imposed macroscopic deformation. To study the influence of these controlling parameters on the macroscopic properties of the model, a dimensionless stress deviation parameter D, which measures the deviation of the macroscopic stresses of the imperfect lattice models from their perfect counterparts, is defined as

$$D = \frac{||\mathbf{\Pi}_{per} - \mathbf{\Pi}_{imp}||}{||\mathbf{\Pi}_{per}||}, \tag{31}$$

where $\mathbf{\Pi}_{per}$ and $\mathbf{\Pi}_{imp}$ are the exact macroscopic first Piola-Kirchhoff stress tensors of the perfectly periodic and the imperfect lattice models, respectively. The limit of the stress deviation parameter as the geometric scale parameter approaches zero is denoted by D_0 (i.e., $D_0 = \lim_{\epsilon \to 0} D$). Scale effects on the macroscopic stress-strain response of the models, which are due to microstructural imperfections, are studied by examining the dependence of this stress deviation parameter D on the geometric scale parameter ϵ. The dependence of the stress deviation limit D_0 on the imperfection amplitude parameter δ and the imposed macroscopic deformation (defined by $\mathbf{F}_0$) are also explored.

The effects of geometric imperfections on the stress deviation parameter are studied first. Figure 5a shows the scale effects, due to microstructural imperfections, on D for a lattice model with regular ($m_1 = m_2 = 1, 2, 3, 4$, depicted by the solid, dashed, dotted, and dashed-dotted lines, respectively) and random geometric imperfections of twenty-five percent amplitude ($\delta = 0.25$), subjected to uniaxial extension with no lateral contraction ($\phi = \theta = 0$ and $\lambda = 0.05$). For models with regular geometric imperfections, the stress deviation parameter converges exponentially to zero as the geometric scale parameter decreases (i.e., $D_0 = 0$). This is expected, since the wavelengths of the imperfection shape are fixed, while the relative size of the imperfection $\delta\epsilon$ decreases to zero. The rate at which the stress deviation

parameter approaches zero decreases as the wave numbers associated with the regular imperfection shape increase. For models with random geometric imperfections, the stress deviation parameter converges to some nonzero asymptotic limit as the geometric scale parameter decreases (i.e., $D_0 \neq 0$). Here, the imperfection wavelengths are of the order of the unit cell dimensions, therefore, the microstructural geometry remains highly irregular, even as the geometric scale parameter decreases. The stress deviation limit D_0 is plotted as a function of the imperfection amplitude parameter δ in Figure 5b for the lattice model with random geometric imperfections. As expected, the results show that the stress deviation limit curve is parabolic ($D_0 \sim |\delta|^2$). Recall that the effects of arbitrary geometric microstructural imperfections on the macroscopic properties of the lattice models are second order in the imperfection amplitude parameter δ, as shown in Appendix B.

The effects of constitutive imperfections on the stress deviation parameter are studied next. Figure 6a shows the scale effects on D, due to microstructural imperfections, for a lattice model with regular ($m_1 = m_2 = 1, 2, 3, 4$, depicted by the solid, dashed, dotted, and dashed-dotted lines, respectively) and random constitutive imperfections of twenty-five percent amplitude ($\delta = -0.25$), subjected to uniaxial extension with no lateral contraction ($\phi = \theta = 0$ and $\lambda = 0.05$). As in the case for models with geometric imperfections, the stress deviation parameters for models with constitutive imperfections converge to asymptotic limits as the geometric scale parameter approaches zero. In this case, however, the limits are all nonzero, and depend on the shape of the imperfection. For models with regular constitutive imperfections with $m_1 = m_2 = 1$, all of the element cross-sectional areas (except those that lie along the boundary of the representative volume) are decreased (since $\delta < 0$) and the overall effect on the macroscopic stress-strain response is first order (hence, the much higher asymptotic limit for the stress deviation parameter). As the wave numbers associated with the regular imperfection shapes increase, the asymptotic limits of the stress deviation parameters approach some constant value. Note that for regular imperfections, this constant value is approached from different directions depending on whether the wave numbers of the corresponding imperfection shape are even or odd (i.e., depending on whether the effects are first order or second order in the imperfection amplitude parameter δ). It is to this same value that the stress deviation parameter converges for models with random constitutive imperfections. The stress deviation limit D_0 is plotted as a function of the imperfection amplitude parameter δ in Figure 6b for a lattice model with regular ($m_1 = m_2 = 1, 2$, depicted by the solid and dashed lines, respectively) and random (dotted line) constitutive imperfections. For the model with $m_1 = m_2 = 1$, the linear curve implies that the effects of these imperfections are first order in the imperfection amplitude parameter. For the model with $m_1 = m_2 = 2$ the parabolic curve implies that the effects are second order. And, for the model with random imperfections, the results indicate that the effects are first order, although the

initial slope is negligible.

It is expected that a given microstructure will have a combination of both geometric and constitutive microstructural imperfections. The stress deviation limit D_0 is plotted as a function of the imperfection amplitude parameter δ in Figure 7 for a lattice model with a combination of random geometric and constitutive imperfections (solid line), subjected to uniaxial extension with no lateral contraction ($\phi = \theta = 0$ and $\lambda = 0.05$). The combined effect of these imperfections is shown to compare closely with the sum of the effects for each imperfection considered separately (dashed-dotted line).

All of the above results are for a given loading direction and a fixed magnitude of strain ($\phi = \theta = 0$ and $\lambda = 0.05$). The influence of the particular load path and magnitude of strain on the stress deviation limit is addressed next. The stress deviation limit D_0 is plotted as a function of the principal stretch ratios λ_1 and λ_2 in Figure 8a for pure biaxial deformations ($\theta = 0$), and in Figure 8b for deformations including shear ($\theta = \pi/8$). For both deformations a lattice model with regular ($m_1 = m_2 = 1$) constitutive imperfections of twenty-five percent amplitude ($\delta = -0.25$) is considered. Both figures show that, for any load path, the stress deviation limit D_0 remains between nine and ten percent for levels of deformation approaching the onset of failure. This implies that the effects of constitutive imperfections on the macroscopic properties are almost insensitive to the state of strain in the lattice models. Similar results are found for constitutive imperfections with random shapes, and for arbitrary geometric imperfections, as well.

The final topic of interest pertains to the accuracy of the proposed analytical approximations. The exact stress-strain response for lattice models with imperfect microstructures is compared to the response predicted by the Voigt and the displacement linearization approximations derived in Section 3.2. To illustrate how well the proposed approximations predict the macroscopic stress-strain response, regular ($m_1 = m_2 = 1$) constitutive imperfections of twenty-five percent amplitude ($\delta = -0.25$) are considered for models with $\epsilon = 0.04$. To quantify the error of the analytical approximations, a stress error measure $\mathcal{D}$, which quantifies the difference between the exact and approximate macroscopic stress tensor norms, is defined as

$$\mathcal{D} = \frac{||\mathbf{\Pi}_{ex} - \mathbf{\Pi}_{app}||}{||\mathbf{\Pi}_{ex}||}, \tag{32}$$

where $\mathbf{\Pi}_{ex}$ and $\mathbf{\Pi}_{app}$ are the exact and approximate macroscopic stress tensors of the imperfect lattice models, respectively.

The approximations are analyzed for a lattice model subjected to a series of boundary conditions encompassing both pure biaxial deformations and deformations including shear. The stress error measure $\mathcal{D}$ for the Voigt approximation is plotted as a function of the principal stretch ratios λ_1 and λ_2 in Figure

9a for pure biaxial deformations ($\theta = 0$), and in Figure 9b for deformations including shear ($\theta = \pi/8$). The stress error measure for the displacement linearization approximation is shown in Figure 10a for pure biaxial deformations, and in Figure 10b for deformations including shear. The results show that the errors for both approximations are less than one percent, for models with relatively large imperfection amplitude parameters, and for a broad range of macroscopic strains approaching the onset of failure. The displacement linearization approximation is found to be more accurate than the Voigt approximation by roughly an order of magnitude. The accuracy of both approximations improves even further as the imperfection amplitude parameter decreases, or as the imperfection shape changes resulting in the smaller, second order ($O(\delta^2)$) effects.

This section is concluded with a note on the computational efficiency and the corresponding usefulness of the proposed approximation methods. Recall, that to obtain the stress state of an imperfect lattice model at a finite level of strain, many numerical solutions (one for each increment along the particular load path) involving the entire micromechanical model are required. The proposed approximation methods, on the other hand, require only one solution involving the entire model, to determine the displacement correction terms due to the imperfection. Moreover, the assembly of the corresponding stiffness matrix, for the entire lattice model, only requires information about the state of the unit cell at the strain level in question. These computational advantages become important in the case of microstructured continua, where the size and the complexity of the models are orders of magnitude higher.

5 CONCLUSIONS

The present work addresses the influence of scale on the macroscopic properties of nonlinearly elastic materials under finite macroscopic strain. Of interest here are materials with periodic and nearly periodic microstructures, for which a geometric scale parameter ϵ can be unambiguously defined as the ratio of the unit cell size, to the overall size of the representative volume. In the interest of computational efficiency, a kinematically and constitutively nonlinear lattice is proposed as the basic model for this investigation. The results from the present simple nonlinear truss model are indicative of the behavior of more realistic (both in the geometric and constitutive sense) solids.

The macroscopic properties of a perfectly periodic lattice model, subjected to a uniform macroscopic strain field, are independent of the geometric scale parameter ϵ. The scale effect on the macroscopic properties of the model are due either to nonuniformities in the imposed macroscopic strain field, or to the presence of geometric or constitutive microstructural imperfections. The influence of scale on the exact macroscopic properties under these two conditions is investigated, and analytical methods are proposed in each case to approximate these effects.

Regarding the influence of macroscopic strain nonuniformities on the macroscopic properties, previous work has shown that the $O(\epsilon^2)$ correction to the average macroscopic strain energy density is not unique, and that the various corrections differ by a null Lagrangian (see Bardenhagen and Triantafyllidis, 1994). The present work, which is based on exact calculations involving the strain energy density of the representative volume, clarifies this ambiguity by showing which of these correction terms is appropriate. Consequently, the proper expression for the macroscopic strain energy density, which is correct to $O(\epsilon^2)$, involves only the gradient of the macroscopic strain ($\mathbf{F} \otimes \nabla$), which is the form selected for most empirical calculations in nonlinear solids, where scale effects have to be included (see the discussion in Bardenhagen and Triantafyllidis, 1994).

Concerning both geometric and constitutive microstructural imperfections, the influence of scale, imperfection amplitude, and imperfection shape have all been investigated by examining the dependence of the dimensionless stress deviation parameter D on the corresponding geometric scale and imperfection parameters (i.e., on ϵ, δ, m_1, and m_2). It is shown that geometric imperfections produce a second order ($O(\delta^2)$) effect on the macroscopic properties, while constitutive imperfections produce either a first order or second order effect, according to whether or not the imperfection changes the average initial stiffness of the lattice model (i.e., according to whether the wave numbers of the corresponding imperfection shape are odd or even, respectively).

The investigation is concluded by proposing two different approximation methods for calculating

the macroscopic properties of the imperfect lattice models (a straightforward averaging and a direct linearization method). The accuracies of these approximation methods are verified for all macroscopic strains (up to the onset of failure in the model), and both methods are shown to be highly precise, even for large imperfection amplitudes, and are shown to be insensitive to the magnitude and orientation of the macroscopic strain.

All of the results of this investigation are valid for finite strains smaller than those corresponding to the onset of failure in the representative volume of the model. The issues of defining a failure surface in macroscopic strain space for these models, and the dependence of this failure surface on the relative size of the specimen under investigation, is the topic of Part II of this work.

ACKNOWLEDGMENTS

The present work was partially funded, initially by Alcoa, and subsequently by AFOSR under Grant DOD-G-F49620-94-1-0402. The authors would like to express their appreciation for this financial assistance, and their gratitude to Dr. Owen Richmond of the Alcoa Technical Center for his interest and encouragement, and for sharing his ideas on the subject of stability as it relates to microstructured materials.

References

[1] Bardenhagen, S. and Triantafyllidis, N. (1994) Derivation of higher order gradient continuum theories in 2,3-D non-linear elasticity from periodic lattice models. *J. Mech. Phys. Solids* **42**, 111-139.

[2] Born, M. and Huang, K. (1954) *Dynamical Theory of Crystal Lattices* (Chapter 3). Oxford University Press, Oxford.

[3] Drugan, W. J. and Willis, J. R. (1996) A micromechanics-based nonlocal constitutive equation and estimates of representative volume element size for elastic composites. *J. Mech. Phys. Solids* **44**, 497-524.

[4] Hill, R. (1965) Continuum micro-mechanics in elastoplastic polycrystals. *J. Mech. Phys. Solids* **13**, 89-101.

[5] Kunin, I. A. (1982) *Elastic Media with Microstructure I, One-Dimensional Models*. Springer, Berlin.

[6] Triantafyllidis, N. and Bardenhagen, S. (1993) On higher order gradient continuum theories in 1-D nonlinear elasticity. Derivation from and comparison to the corresponding discrete models. *J. Elasticity* **33**, 259-293.

[7] Triantafyllidis, N. and Bardenhagen, S. (1996) The influence of scale size on the stability of periodic solids and the role of associated higher order gradient continuum models. *J. Mech. Phys. Solids* **44**, 1891-1928.

[8] Voigt, W. (1889) Über die Beziehung zwischen den beiden Elastizitätskonstanten isotroper Körper, *Wied. Ann.*, Vol. 38, 573-587.

[9] Talbot, D. R. S. and Willis, J. R. (1985) Variational principles for nonlinear inhomogeneous media. *IMA J. Appl. Math.* **35**, 39-54.

APPENDIX A: STRAIN ENERGY DENSITY CONVERGENCE RESULT IN 1–D

Of interest here, is the derivation of the second order ($O(\epsilon^2)$) correction to the strain energy density of the lattice model. The expansion of the exact strain energy density W, in terms of ascending powers of the geometric scale parameter ϵ, can be written as

$$W = W_0 + \frac{\epsilon^2}{2} W_2 + O\left(\epsilon^4\right), \tag{33}$$

where the $O\left(\epsilon^0\right)$ term, $W_0 = (1/L)\int_0^L W dX$ is the average strain energy density. Here, the absence of any odd order terms in the geometric scale parameter ϵ (i.e., W_1, W_3, ...) is due to the symmetry of the microstructure. Of interest is the limit of the second order term W_2 (which is the lowest order term in the macroscopic strain energy density which contains scale information) as the geometric scale parameter ϵ approaches zero.

From equation (33), the second order term W_2 is defined as

$$W_2 = \lim_{\epsilon \to 0} \left[\frac{W - (1/L)\int_0^L W dX}{\epsilon^2/2} \right] = \frac{1}{L} \int_0^L \left[\frac{\epsilon W_i - \int_{X_i}^{X_{i+1}} W dX}{\epsilon^3/2} \right] dX, \tag{34}$$

where $W_i = W\left(e_i\left(X\right)\right)$ is the strain energy density of element i, $e_i\left(X\right)$ is the strain of element i, and X_i and X_{i+1} are the reference positions for the element nodes.

Let the displacement of each node correspond to a continuous, macroscopic deformation gradient $F\left(X\right)$ such that

$$u = \left(F_0 - 1\right) X + \frac{1}{2} F_1 X^2 + \frac{1}{6} F_2 X^3. \tag{35}$$

Here, $F_0 = (1/L)\int_0^L F\left(X\right) dX$ is the average macroscopic deformation gradient, and F_1 and F_2 are second and third order deformation gradients, respectively.

Using equation (35) for the displacements, the element strains can be written as

$$e_i\left(X\right) = \frac{u\left(X_{i+1}\right) - u\left(X_i\right)}{\epsilon} = \frac{\partial u\left(X_{i+1/2}\right)}{\partial X} + \frac{\epsilon^2}{24} F_2. \tag{36}$$

Substitution of the element strain relation (36) into $W\left(e_i\left(X\right)\right)$ and subsequent expansion yields

$$W\left(e_i\left(X\right)\right) = W\left(e\left(X_i\right)\right) + \frac{\epsilon}{2} \frac{dW\left(e\left(X_i\right)\right)}{dX} + \frac{\epsilon^2}{8} \frac{d^2 W\left(e\left(X_i\right)\right)}{dX^2} + \frac{\epsilon^2}{24} \frac{dW\left(e\left(X_i\right)\right)}{de} F_2. \tag{37}$$

Expansion of $\int_{X_i}^{X_{i+1}} W\left(e\left(X\right)\right) dX$ yields

$$\int_{X_i}^{X_{i+1}} W\left(e\left(X\right)\right) dX = \epsilon W\left(e\left(X_i\right)\right) + \frac{\epsilon^2}{2}\frac{dW\left(e\left(X_i\right)\right)}{dX} + \frac{\epsilon^3}{6}\frac{d^2W\left(e\left(X_i\right)\right)}{dX^2}. \tag{38}$$

And finally, substitution of the expansions (37) and (38) into the relation for the second order strain energy density term (34), and subsequent simplification gives

$$W_2 = \frac{1}{L}\int_0^L \left[-\frac{1}{12}\frac{d^2W}{de^2}\left(\frac{\partial^2 u}{\partial X^2}\right)^2\right] dX, \tag{39}$$

which can be written as

$$W_2 = \frac{1}{L}\int_0^L \left[\frac{\partial^2 u}{\partial X^2} B \frac{\partial^2 u}{\partial X^2}\right] dX, \qquad \text{where} \qquad B = -\frac{1}{12}\frac{\partial^2 W}{\partial e^2}. \tag{40}$$

The additional term included in equation (23) involving $\partial \mathcal{E}^{el}/\partial \overline{e}^{el}$ results from using the nonlinear Lagrangian strain measure defined by equation (22). The remaining differences between equations (23) and (40) are due to the fact that only a one-dimensional model was considered here.

APPENDIX B: EFFECTS OF GEOMETRIC IMPERFECTIONS ON THE MACROSCOPIC PROPERTIES

Of interest here, are the effects of geometric microstructural imperfections on the macroscopic properties, and in particular the dependence of these properties on the imperfection amplitude parameter δ. To determine this dependence, the expansion of the exact strain energy density of the lattice model is considered. The first order term in the expansion of the strain energy density is

$$W_1 = \left.\frac{dW}{d\delta}\right|_{\delta=0} = \left.\left(\frac{\partial W}{\partial \delta} + \frac{\partial W}{\partial \mathbf{u}}\cdot\frac{\partial \mathbf{u}}{\partial \delta}\right)\right|_{\delta=0}. \tag{41}$$

Consider a planar lattice model with arbitrary geometric microstructural imperfections. For this model, it can be shown, after some lengthy but straightforward algebra (which takes into account the fact that the boundary nodes are unperturbed), that

$$\left.\frac{\partial W}{\partial \delta}\right|_{\delta=0} = 0. \tag{42}$$

Also, from the equilibrium equations,

$$\delta\mathbf{u}\cdot\frac{\partial \mathcal{E}}{\partial \mathbf{u}} = 0 \qquad \text{in} \qquad V \qquad \text{and} \qquad \delta\mathbf{u} = \mathbf{0} \qquad \text{on} \qquad \partial V, \tag{43}$$

it follows that

$$\frac{\partial W}{\partial \mathbf{u}}\cdot\frac{\partial \mathbf{u}}{\partial \delta} = 0, \tag{44}$$

since $\partial\mathbf{u}/\partial\delta$ is a kinematically admissible field (i.e., $\mathbf{u} = (\mathbf{F}_0 - \mathbf{I})\cdot\mathbf{X}$ on $\partial V \Rightarrow \partial\mathbf{u}/\partial\delta = \mathbf{0}$ on ∂V).

From equations (43) and (45), it follows that for lattice models with arbitrary geometric microstructural imperfections, the first order term in the expansion of the exact strain energy density W_1 is identically zero. And, since $\mathbf{\Pi}^T = \partial W/\partial \mathbf{F}_0$ and $\mathbf{L} = \partial^2 W/\partial \mathbf{F}_0 \partial \mathbf{F}_0$, it follows that

$$\mathbf{\Pi}_1 = \mathbf{0} \qquad \text{and} \qquad \mathbf{L}_1 = \mathbf{0}, \tag{45}$$

for deformations satisfying the prescribed displacement boundary conditions. Therefore, the effects of arbitrary geometric imperfections are second order in the imperfection amplitude parameter δ.

APPENDIX C: $O(\delta)$ COINCIDENCE OF THE VOIGT AND LINEARIZATION APPROXIMATIONS

Of interest here, is the comparison of the predictions for the macroscopic properties obtained using the Voigt and the standard linearization approximations. Consider a planar lattice model with arbitrary geometric or constitutive microstructural imperfections. Recall that the macroscopic strain energy density, as given by the Voigt approximation, is

$$\overline{W}_V = W\left(\delta, \mathbf{u}_0\right) = W|_{\delta=0} + \delta \left.\frac{\partial W}{\partial \delta}\right|_{\delta=0} + O(\delta^2), \tag{46}$$

and the strain energy density, as given by the linearization approximation, is

$$\overline{W}_L = W|_{\delta=0} + \delta \left.\frac{dW}{d\delta}\right|_{\delta=0} = W|_{\delta=0} + \delta \left.\left(\frac{\partial W}{\partial \delta} + \frac{\partial W}{\partial \mathbf{u}} \cdot \frac{\partial \mathbf{u}}{\partial \delta}\right)\right|_{\delta=0}. \tag{47}$$

From the equilibrium equations, it follows that

$$\frac{\partial W}{\partial \mathbf{u}} \cdot \frac{\partial \mathbf{u}}{\partial \delta} = 0. \tag{48}$$

Therefore, the strain energy density, as given by the linearization approximation, becomes

$$\overline{W}_L = W|_{\delta=0} + \delta \left.\frac{\partial W}{\partial \delta}\right|_{\delta=0}, \tag{49}$$

which differs from the strain energy density as given by the Voigt method $\overline{W}_V$ by $O(\delta^2)$. Similar results hold for the average stresses and incremental moduli tensors.

FIGURE CAPTIONS

Figure 1: The discrete, planar, lattice model. (a) Perfectly periodic microstructure with geometric scale parameter $\epsilon = h/H = 0.1$. (b) Nondimensional force-elongation response for the base element of the unit cell with $\mathcal{A} = 1$, $E = 1$, $a = -7/2$ and $b = 7/2$.

Figure 2: Reference configurations for a planar lattice model with $\epsilon = 0.1$ and (a) regular ($m_1 = m_2 = 2$) and (b) random geometric imperfections of twenty-five percent amplitude ($\delta = 0.25$).

Figure 3: (a) Scale effects, due to nonuniform deformations, on the exact strain energy density of a perfectly periodic lattice model. (b) Corresponding convergence of the function $f(\epsilon)$ to one as the geometric scale parameter ϵ approaches zero.

Figure 4: Effects of regular ($m_1 = m_2 = 1$) and random constitutive imperfections of twenty-five percent amplitude ($\delta = -0.25$) on the macroscopic stress-strain response of an initially perfectly periodic lattice model with $\epsilon = 0.04$, subjected to uniaxial extension with no lateral contraction ($\phi = \theta = 0$).

Figure 5: (a) Scale effects, due to microstructural imperfections, on the stress deviation parameter D for a lattice model with regular and random geometric imperfections of twenty-five percent amplitude ($\delta = 0.25$), subjected to uniaxial extension with no lateral contraction ($\phi = \theta = 0$ and $\lambda = 0.05$). (b) Corresponding stress deviation limit D_0 as a function of the imperfection amplitude parameter δ.

Figure 6: (a) Scale effects, due to microstructural imperfections, on the stress deviation parameter D for a lattice model with regular and random constitutive imperfections of twenty-five percent amplitude ($\delta = -0.25$), subjected to uniaxial extension with no lateral contraction ($\phi = \theta = 0$ and $\lambda = 0.05$). (b) Corresponding stress deviation limit D_0 as a function of the imperfection amplitude parameter δ.

Figure 7: The stress deviation limit D_0 as a function of the imperfection amplitude parameter δ for a lattice model with random geometric imperfections, random constitutive imperfections, and a combination of random geometric and constitutive imperfections of twenty-five percent amplitude ($\delta = -0.25$), subjected to uniaxial extension with no lateral contraction ($\phi = \theta = 0$ and $\lambda = 0.05$).

Figure 8: The stress deviation limit D_0 as a function of the principal stretch ratios λ_1 and λ_2 for a lattice model with regular ($m_1 = m_2 = 1$) constitutive imperfections of twenty-five percent amplitude ($\delta = -0.25$), subjected to (a) pure biaxial deformations ($\theta = 0$) and (b) deformations including shear ($\theta = \pi/8$).

Figure 9: Voigt approximation stress error measure $\mathcal{D}$ as a function of the principal stretch ratios λ_1 and λ_2 for a lattice model with $\epsilon = 0.04$ and regular ($m_1 = m_2 = 1$) constitutive imperfections of twenty-five

percent amplitude ($\delta = -0.25$), subjected to (a) pure biaxial deformations ($\theta = 0$) and (b) deformations including shear ($\theta = \pi/8$).

Figure 10: Displacement linearization approximation stress error measure $\mathcal{D}$ as a function of the principal stretch ratios λ_1 and λ_2 for a lattice model with $\epsilon = 0.04$ and regular ($m_1 = m_2 = 1$) constitutive imperfections of twenty-five percent amplitude ($\delta = -0.25$), subjected to (a) pure biaxial deformations ($\theta = 0$) and (b) deformations including shear ($\theta = \pi/8$).

FIGURES

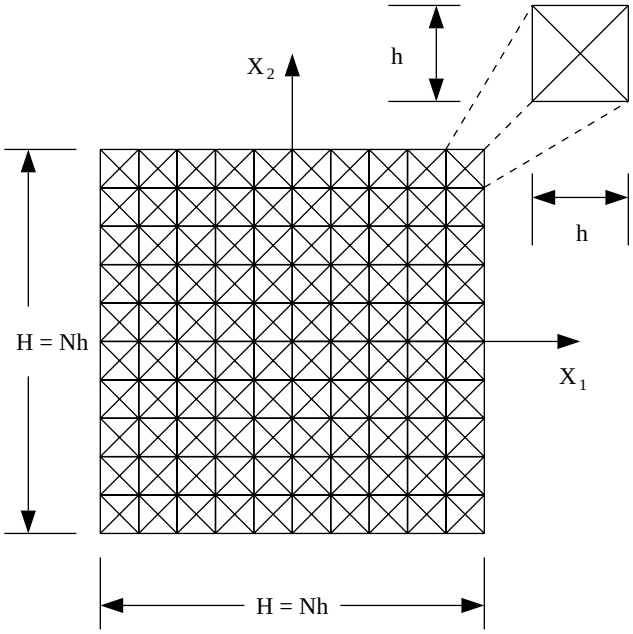

(a)

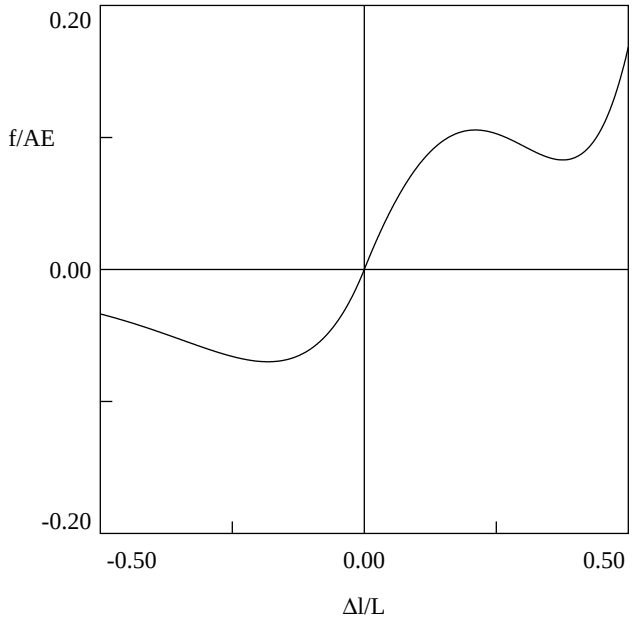

(b)

Figure 1: See FIGURE CAPTIONS

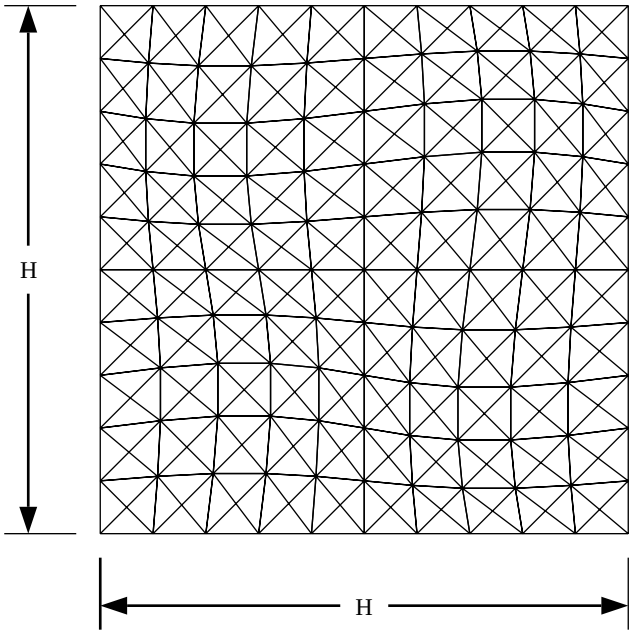

(a)

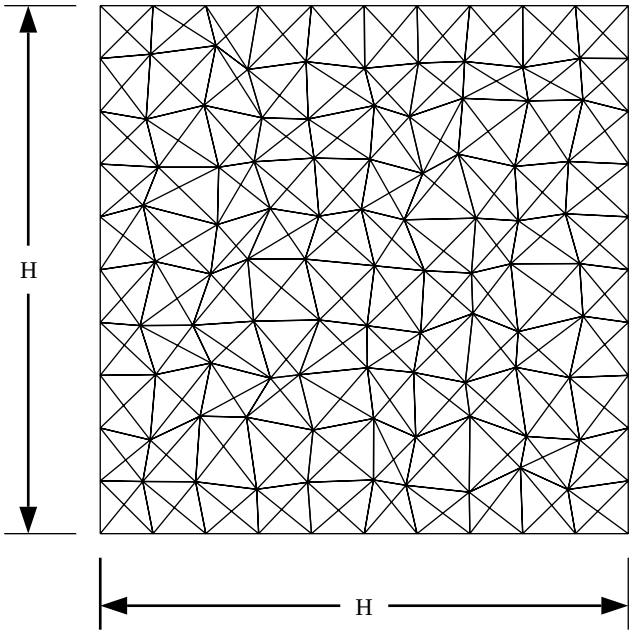

(b)

Figure 2: See FIGURE CAPTIONS

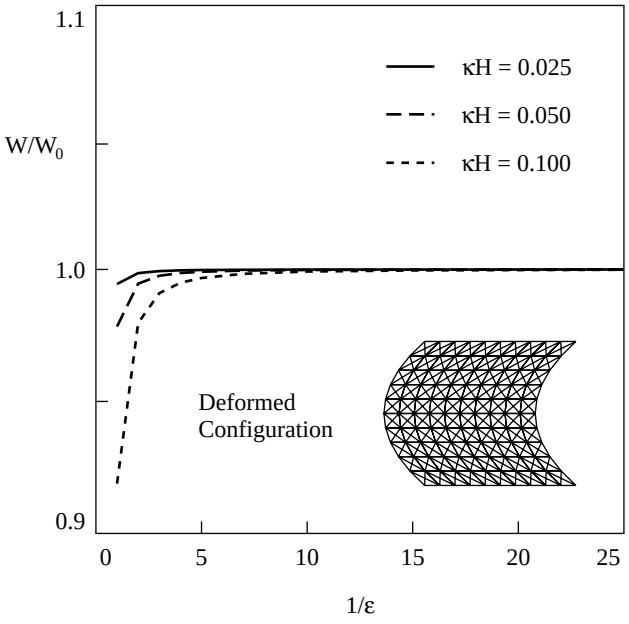

(a)

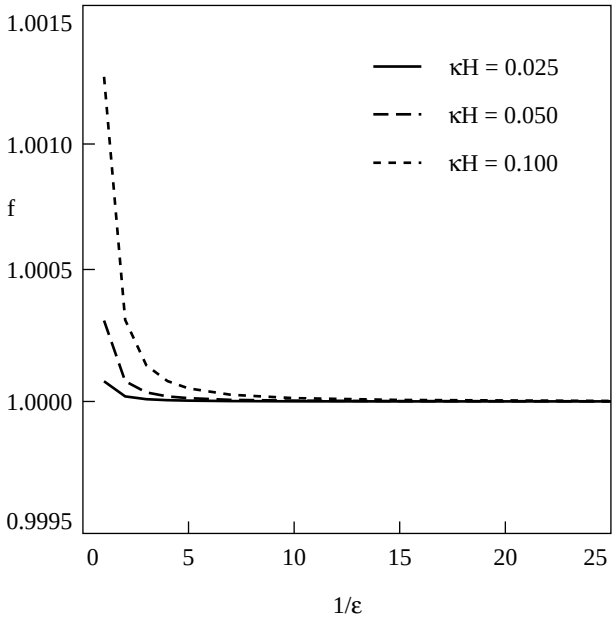

(b)

Figure 3: See FIGURE CAPTIONS

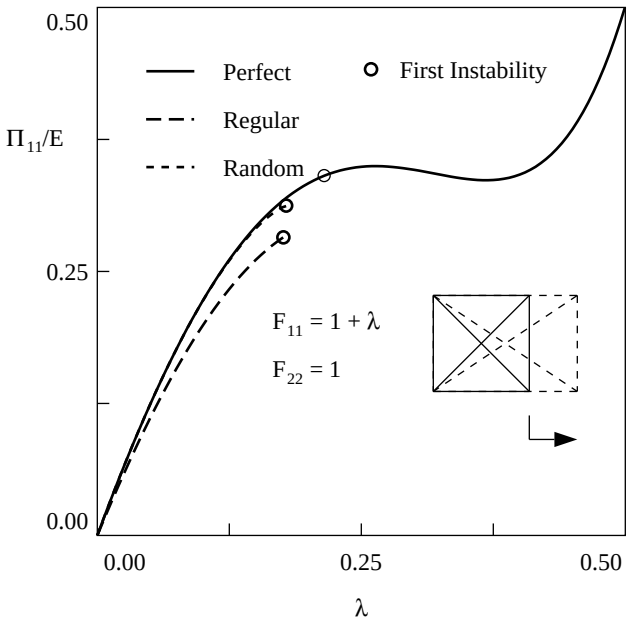

Figure 4: See FIGURE CAPTIONS

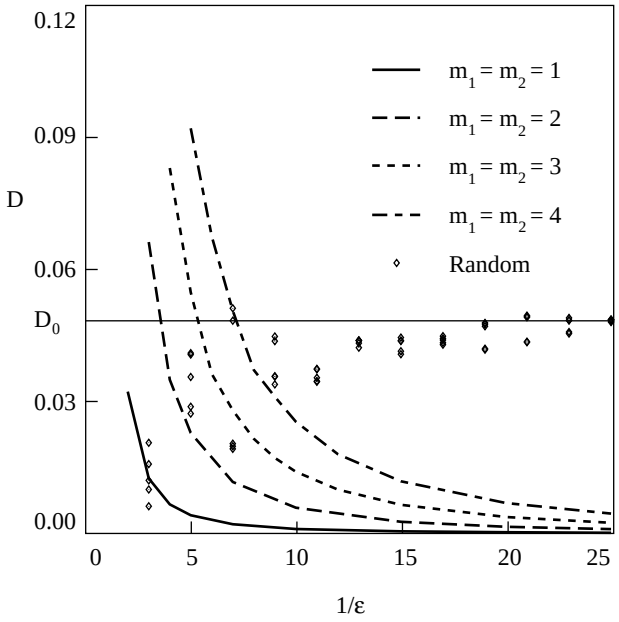

(a)

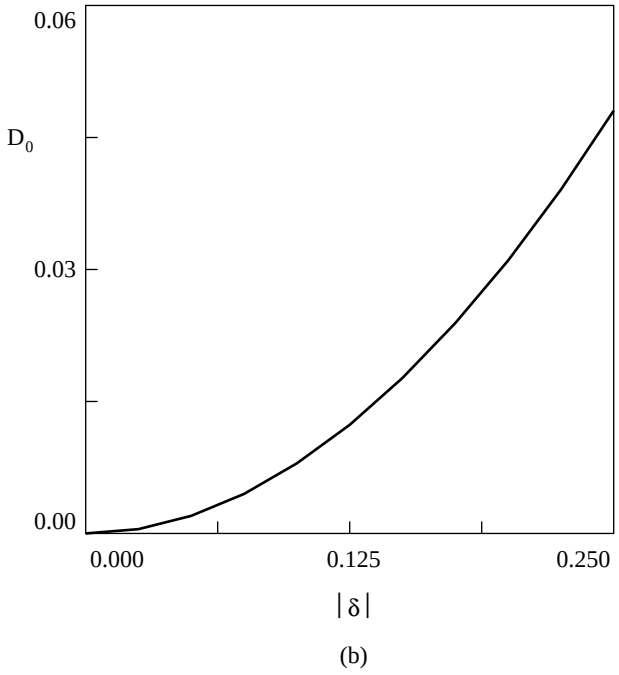

(b)

Figure 5: See FIGURE CAPTIONS

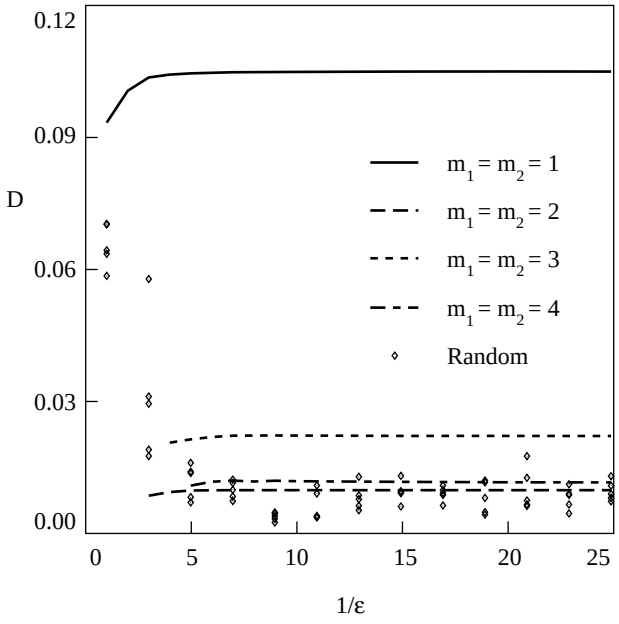

(a)

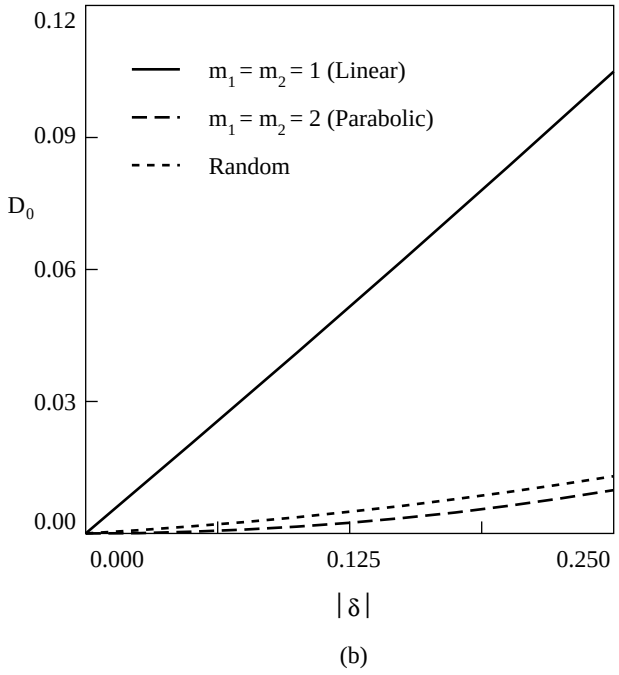

(b)

Figure 6: See FIGURE CAPTIONS

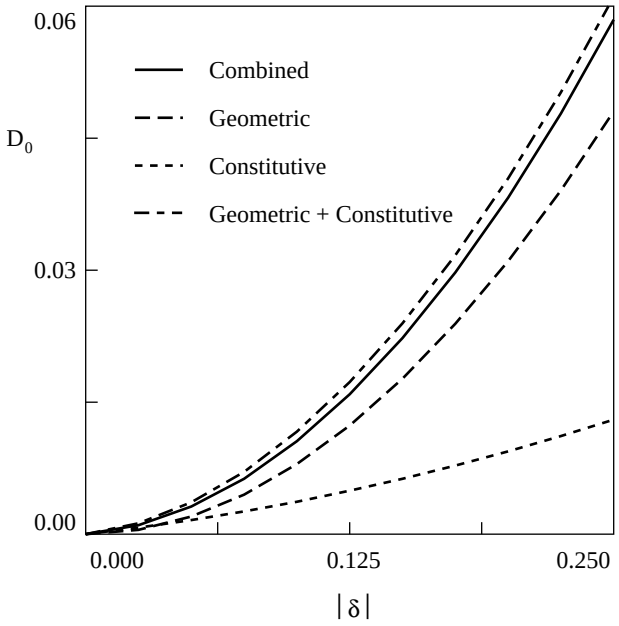

Figure 7: See FIGURE CAPTIONS

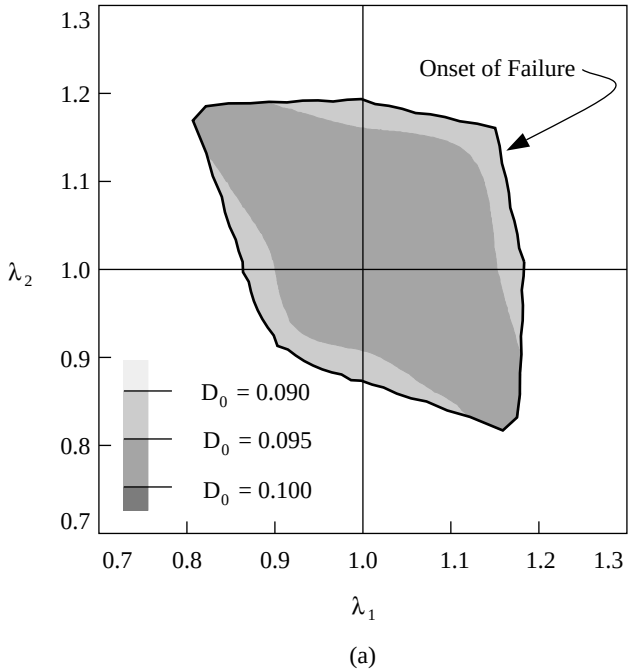

(a)

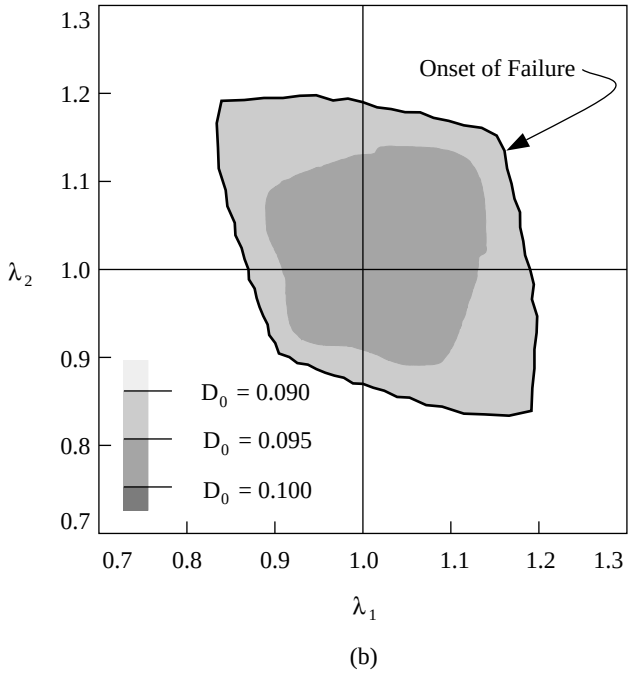

(b)

Figure 8: See FIGURE CAPTIONS

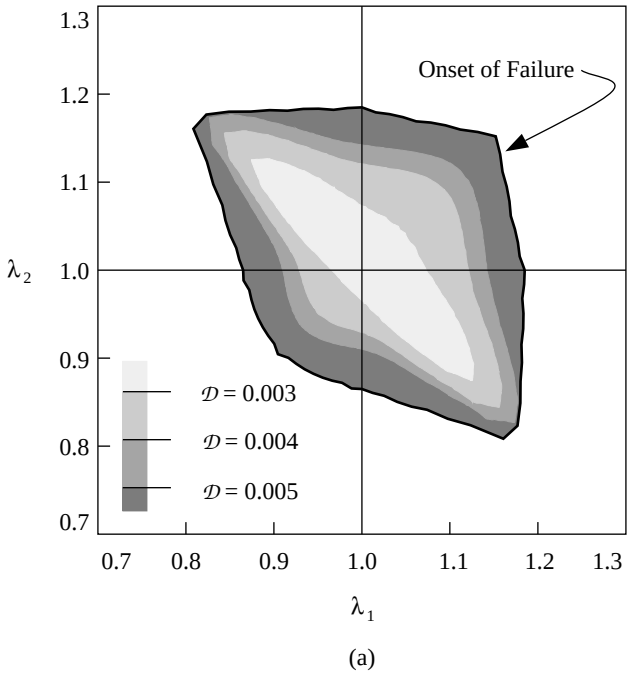

(a)

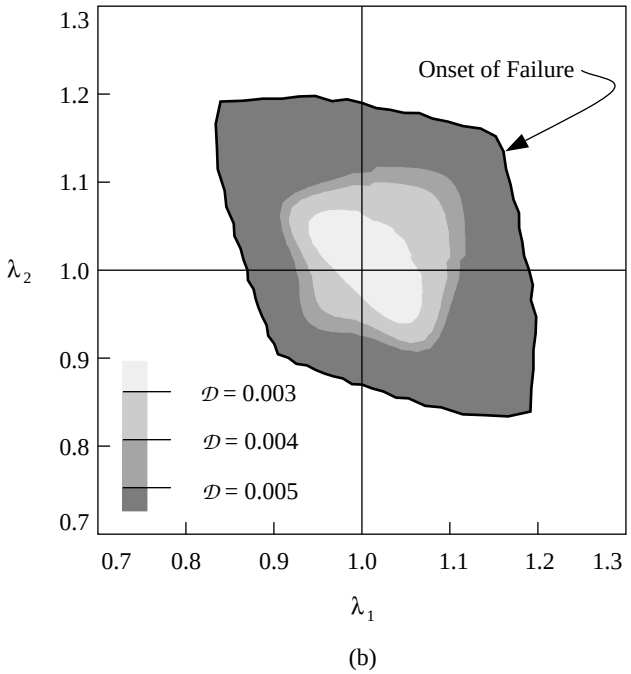

(b)

Figure 9: See FIGURE CAPTIONS

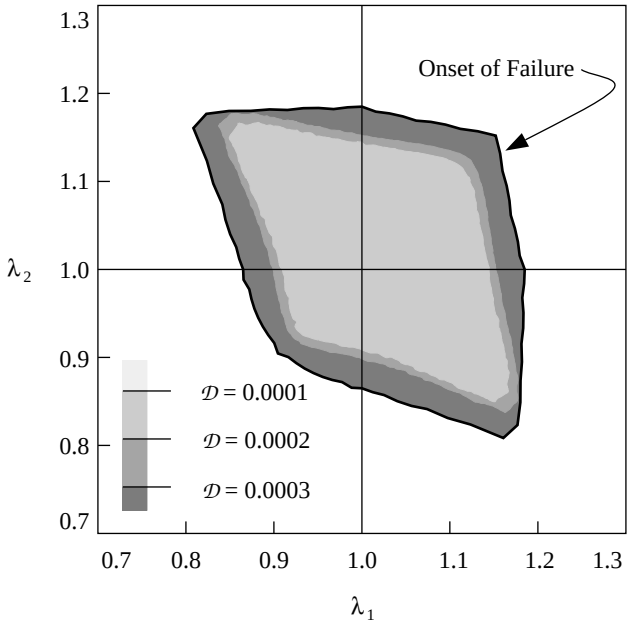

(a)

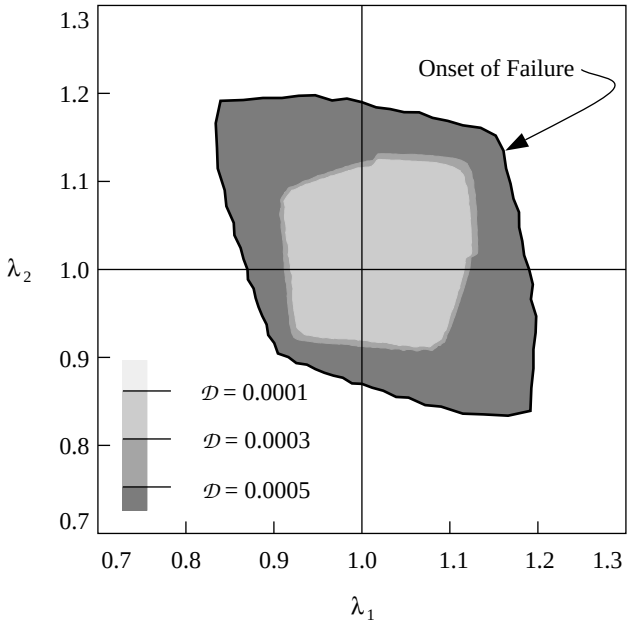

(b)

Figure 10: See FIGURE CAPTIONS